

## Article

# Glucose-Sensing Carbohydrate Response Element-Binding Protein in the Pathogenesis of Diabetic Retinopathy

Christopher R. Starr <sup>1</sup> , Assylbek Zhylykbayev <sup>2</sup> , Oleg Gorbatyuk <sup>3</sup>, Alli M. Nuotio-Antar <sup>4</sup> , James Mobley <sup>5</sup>, Maria B. Grant <sup>1</sup> and Marina Gorbatyuk <sup>2,\*</sup> 

<sup>1</sup> Department of Ophthalmology, School of Medicine, University of Alabama at Birmingham, Birmingham, AL 35233, USA; crstarr@uab.edu (C.R.S.); mabgrant@uab.edu (M.B.G.)

<sup>2</sup> Department of Biochemistry, School of Medicine, Wake Forest University, Winston Salem, NC 27101, USA; azhylykb@wakehealth.edu

<sup>3</sup> Department of Translational Neuroscience, School of Medicine, Wake Forest University, Winston Salem, NC 27101, USA; ogorbaty@wakehealth.edu

<sup>4</sup> Department of Pediatrics, Baylor College of Medicine, Houston, TX 77030, USA; antar@bcm.edu

<sup>5</sup> Department of Anesthesiology and Perioperative Medicine, School of Medicine, University of Alabama at Birmingham, Birmingham, AL 35233, USA; mobleyja@uab.edu

\* Correspondence: mgorbaty@wakehealth.edu

**Abstract:** Glucose-sensing ChREBP and MondoA are transcriptional factors involved in the lipogenic, inflammatory, and insulin signaling pathways implicated in metabolic disorders; however, limited ocular studies have been conducted on these proteins. We aimed to investigate the potential role of ChREBP in the pathogenesis of diabetic retinopathy (DR). We used diabetic human and mouse retinal cryosections analyzed by immunohistochemistry. qRT-PCR was performed to quantify gene expression. To explore the role of ChREBP in rods, we generated caChREBP<sup>RP</sup> mice with constitutively active (ca) ChREBP. These mice underwent retinal functional testing, which was followed by proteomic analysis using LC-MS. Furthermore, ARPE-19 cells were infected with lentiviral particles expressing human ChREBP (ARPE-19<sup>ChREBP</sup>) and subjected to global proteomics. Our results demonstrate that both proteins were expressed across the retina, although with distinct distribution patterns: MondoA was more prominently expressed in cones, while ChREBP was broadly expressed throughout the retina. Elevated expression of both proteins was observed in DR. This may have contributed to rod photoreceptor degeneration, as we observed diminished scotopic ERG amplitudes in caChREBP<sup>RP</sup> mice at P35. The retinal proteomic landscape revealed a decline in the KEGG pathways associated with phototransduction, amino acid metabolism, and cell adhesion. Furthermore, rod-specific caChREBP induced TXNIP expression. Consistent with altered retinal proteomics, ARPE-19<sup>ChREBP</sup> cells exhibit a metabolic shift toward increased glyoxylate signaling, sugar metabolism, and lysosomal activation. Our study demonstrates that ChREBP overexpression causes significant metabolic reprogramming triggering retinal functional loss in mice.

**Keywords:** diabetic retinopathy; ChREBP; MondoA; proteomics



Academic Editors: Mehrnoosh Saghizadeh Ghiam and Vivien Coulson-Thomas

Received: 4 December 2024

Revised: 31 December 2024

Accepted: 7 January 2025

Published: 13 January 2025

**Citation:** Starr, C.R.; Zhylykbayev, A.; Gorbatyuk, O.; Nuotio-Antar, A.M.; Mobley, J.; Grant, M.B.; Gorbatyuk, M. Glucose-Sensing Carbohydrate Response Element-Binding Protein in the Pathogenesis of Diabetic Retinopathy. *Cells* **2025**, *14*, 107. <https://doi.org/10.3390/cells14020107>

**Copyright:** © 2025 by the authors. Licensee MDPI, Basel, Switzerland.

This article is an open access article distributed under the terms and conditions of the Creative Commons Attribution (CC BY) license (<https://creativecommons.org/licenses/by/4.0/>).

## 1. Introduction

Glucose sensing Mondo family proteins (MFPs), carbohydrate response element-binding protein (ChREBP), and MondoA are transcriptional modulators of lipogenic, inflammatory, and insulin signaling-associated genes that are compromised in diabetic retinopathy (DR). Both MFPs exist as heterodimers that form complexes with Max-like protein X (MLX) [1,2]. In response to increased glucose flux into cells, both MFPs translocate to

the nucleus where they independently bind the MLX transcription factor, activating gene expression via the ChoRE element within the promoters of target genes [3]. Examples of such genes include thioredoxin-interacting protein (TXNIP) and Arrestin Domain-Containing Protein 4 (ARRDC4) [3,4]. While current research suggests their overlapping roles in the regulation of lipid metabolism and TXNIP-mediated activation of nucleotide-binding domain, leucine-rich repeat, and pyrin domain-containing protein 3, mounting evidence indicates their independent roles in different tissues. Thus, MondoA primarily drives lipid metabolism and insulin signaling along with the control of ARRDC4-mediated glucose uptake [5,6], while ChREBP controls de novo lipogenesis and glycolysis [7,8]. ChREBP is primarily expressed in the pancreas, adipose tissue, and liver, whereas MondoA is predominantly found in skeletal muscle and immune cells [9]. For instance, in mice challenged with a high-fat diet, liver-specific ChREBP overexpression leads to elevated serum triglycerides and increased inflammation [10,11]. A muscle-specific MondoA knockout, on the other hand, shows reduced expression of genes associated with insulin signaling and fatty acid metabolism [5].

ChREBP has two known functional isoforms,  $\alpha$  and  $\beta$ , each with its own promoter and transcription start site [12]. The ChREBP $\alpha$  protein senses glucose via the activation of two domains: a low-glucose inhibitory domain and a glucose-response activation conserved element domain [13]. Under low-glucose conditions, the low-glucose inhibitory domain inhibits the glucose-response activation conserved element domain, resulting in cytoplasmic retention of ChREBP $\alpha$ . However, under conditions of increased glucose flux into the cell, the intramolecular inhibition of the low-glucose inhibitory domain is reversed, allowing for ChREBP $\alpha$  translocation to the nucleus, where it transactivates target genes, including ChREBP $\beta$ . ChREBP $\beta$  lacks the low-glucose inhibitory domain, making it constitutively active [12].

Previous research has thoroughly investigated the roles of both MFPs in human metabolic disorders. However, only a limited number of ocular studies have focused on ChREBP, and no studies have been conducted on MondoA, indicating a gap in the knowledge on these proteins in the retina [14,15]. It has been proposed that ChREBP-mediated hypoxia-inducible factor 1 (HIF-1 $\alpha$ ) activation may be partially responsible for neovascularization in diabetic and age-related retinopathy [15]. Furthermore, ChREBP deficiency has been shown to reduce high-glucose-induced apoptosis, migration, and tube formation in human retinal microvascular endothelial cells as well as structural and angiogenic responses in the mouse retina [14].

Therapeutic approaches targeting ChREBP and MondoA have recently been proposed to control metabolic disorders [5]. The small-drug inhibitor SBI-993, which deactivates transcription factors ChREBP and MondoA, was shown to reduce liver- and muscle-produced triglycerides, suppress TXNIP and ARRDC4, enhance insulin signaling, and improve glucose tolerance in high-fat-diet-fed mice. This underscores the key roles of these proteins in controlling lipid balance, blood glucose levels, and insulin signaling [6]. These studies also suggest that both ChREBP and MondoA could be targeted therapeutically in ocular conditions. However, it remains to be determined which specific retinal diseases and cell types would benefit from this approach.

## 2. Materials and Methods

### 2.1. Mice

Male C57BL/6J (Strain#: 000664), Akita (Strain #:003548), db/db (BKS.Cg-Dock7m +/+ Leprdb/J; Strain#: 000642), and i-Cre (Strain#: 015850) mice were obtained from the Jackson Laboratory. The eGFP<sup>flox/wt</sup>-caChREBP mice have been described previously [11]. eGFP<sup>flox/wt</sup>-caChREBP mice were bred with i-Cre mice to generate rod photoreceptor (RP)-

specific caChREBP<sup>RP</sup> experimental mice and eGFP<sup>flox/wt</sup>-caChREBP (caChREBP<sup>flox/wt</sup>) littermate controls. All mice were kept in a 12 h light–dark cycle with ad libitum access to food and water. All mice were housed in the University of Alabama at Birmingham (UAB) animal facility, adhering to the guidelines set by the institutional animal care and use committee (UAB-IACUC protocol no. 22104) and the Association for Research in Vision and Ophthalmology guidelines. The animals were euthanized by carbon dioxide followed by cervical dislocation.

## 2.2. Retinal Explants

The eyes from C57BL/6J mice at postnatal day 8 were enucleated, and the retina was gently isolated from the eyecup and placed in Neurobasal Serum-free medium (Neurobasal-A, 10888022; Invitrogen, Waltham, MA, USA) containing 2% B27 (0080085-SA; Invitrogen), 1% N2 (17502-048; Invitrogen), 2 mM GlutaMAX (35050038; Invitrogen), and 100 units/mL penicillin–100 lg/mL streptomycin (P4333; Sigma-Aldrich Corp., St. Louis, MO, USA). Retinal explants were maintained at 37 °C and 5% CO<sub>2</sub>. Mannitol (19 mM; Control) (M4125, Sigma) and D-glucose (34 mM; High glucose) (G5767, Sigma) were dissolved in growth medium. Explants were cultured for 24 h and analyzed using qRT-PCR. All primers were ordered from Sigma-Aldrich Corp. Primers for ChREBP $\alpha$  (forward: 5'-CGACACTCACCCACCTCTTC-3'; reverse: 5'-TTGTTTCAGCCGGATCTTGTC-3'), ChREBP $\beta$  (forward: 5'-TCTGCAGATCGCGTGGAG-3'; reverse: 5'-CTTGTCCCCGGCATAGCAAC-3'), MondoA (forward: 5'-TGCTACCTGCCACAGGA GTC-3'; reverse: 5'-GACTCAAACAGTGGCTTGATGA-3'), and GAPDH (forward: TGACGT-GCCGCCTGAAGAAA; reverse: AGTGTAGCCCAAGATGCCCTTCAG) were used to detect Mondo Family Proteins in the retina. The same primers were applied in the study of diabetic retinas in mice with T1D and T2D.

## 2.3. Infection of Human ARPE-19

With lentiviral particles expressing ChREBP (Cat#: RC220626L2V OriGene Co., Rockville, MD, USA) was conducted using 100  $\mu$ l of suspension. Forty-eight hours later, the ARPE-19<sup>ChREBP</sup> and control cells were harvested, and the protein extracts were prepared for the global proteomic study.

## 2.4. Retinal Tissue and Cell Homogenization and Extraction for Mass Spectrometry

This method was broadly described in our previous study [16]. Briefly, individual retinas and ARPE-19 cells were homogenized. After the samples were trypsinized, they were loaded onto a 1260 infinity high-performance liquid chromatography stack (Agilent Technologies, Santa Clara, CA, USA) and separated using a 75-micron i.d.  $\times$  cm pulled-tip C-18 column (Jupiter C18 300 Å, 5 microns, Phenomenex, Torrance, CA, USA). We used a Thermo Q Exactive HF-X mass spectrometer equipped with a Nanospray Flex ion source (Thermo Fisher Scientific, Waltham, MA, USA) to conduct proteomic analysis. We then analyzed the data using the Shiny Go web resource <http://bioinformatics.sdstate.edu/go/> (accessed on 1 September 2024).

## 2.5. Immunohistochemistry

Human and mouse cryopreserved eyes were cut into sections 12  $\mu$ m thick using a Leica CM1510S cryostat (Leica, Buffalo Grove, IL, USA). The immunohistochemical analysis was conducted on the retinal sections using anti-ChREBP (NB 400-135, Novus Biologicals, Centennial, CO, USA) and anti-MondoA (PA5-23734, Invitrogen) antibodies (dilution 1:200). Donkey anti-Rabbit IgG and Alexa Fluor 488 (A21206, Invitrogen) were employed as secondary antibodies. Imaging analysis was conducted using a BZ-X800 fluorescence microscope (Keyence, Itasca, IL, USA).

## 2.6. Immunoblotting

Mouse retinas were gently isolated and sonicated in a RIPA buffer supplemented with 1% Halt Protease Inhibitor and a phosphatase inhibitor cocktail (78440, Thermo Fisher Scientific). Western blot techniques described in a previous study were employed for further analysis. Protein samples (40–60 µg) were separated by SDS-PAGE and transferred to a PVDF membrane. The anti-TXNIP (VDUP1) (dilution 1:1000, mouse mAb, K0205-3, MBL Life science, Carlsbad, CA, USA) and anti-beta actin (rabbit, A2066, Sigma-Aldrich Corp., dilution 1:5000) antibodies were used for target protein detection. Horseradish peroxidase conjugated Goat anti-Rabbit IgG (926-80011) and goat anti-Mouse IgG (926-80010) from Li-COR Biosciences (Lincoln, NE, USA) were used as secondary antibodies (1:10,000). Images of membranes were captured and analyzed using the Odyssey XF system (Li-COR Biosciences).

## 2.7. Electrophoretography (ERG)

At postnatal (p) day 35, mice were dark-adapted overnight, and all procedures were conducted in a dark room with light adaptation for photopic response using a UTAS BigShot instrument (LKC Technologies, Gaithersburg, MD, USA). We applied 2.5% phenylephrine (42702–102-15, Paragon BioTeck, Inc., Portland, OR, USA) and Gonak (2.5% sterile hypromellose ophthalmic demulcent solution, Alcon, Lake Forest, CA, USA) to the cornea for dilation and to moisturize the ocular surface. For scotopic ERG, mice were exposed to a series of 5 flashes at various intensities, 0.025 cds/m<sup>2</sup> (−20 dB), 2.5 cds/m<sup>2</sup> (0 dB), and 25 cds/m<sup>2</sup> (10 dB), with 45 s intervals between flashes. Following the scotopic protocol, each mouse was light-adapted for 5 min under a dome background light of 25 cds/m<sup>2</sup>. The photopic protocol involved a series of 15 flashes with 1 s intervals between each flash, at intensities of 25 cds/m<sup>2</sup> and 79 cds/m<sup>2</sup>. The obtained results were analyzed using LKC EM software (LKC Technologies, Gaithersburg, MD, USA).

## 2.8. RNAscope

RNAscope was performed in 12-week-old db/db mice according to the manufacturer's (Advanced Cell Diagnostics, Newark, CA, USA) recommendations. ChREBP was analyzed using a probe specific to its mRNA (558141-C3, ACDBio, Newark, CA, USA).

## 2.9. Statistical Analysis

A Student two-tailed paired *t*-test and two-way ANOVA were used to compare the two groups using GraphPad Prism 10.3.1 (509) software. All statistical data were expressed as mean ± SE. *p* < 0.05 was considered significant.

# 3. Results

## 3.1. Mondo Family Proteins, ChREBP and MondoA, Are Upregulated in Human and Mouse Diabetic Retinas

We first sought to localize ChREBP and MondoA in the retina under normal and diabetic conditions. Control and diabetic human retinas were stained with antibodies against ChREBP and MondoA and examined via confocal microscopy (Figure 1A,B).



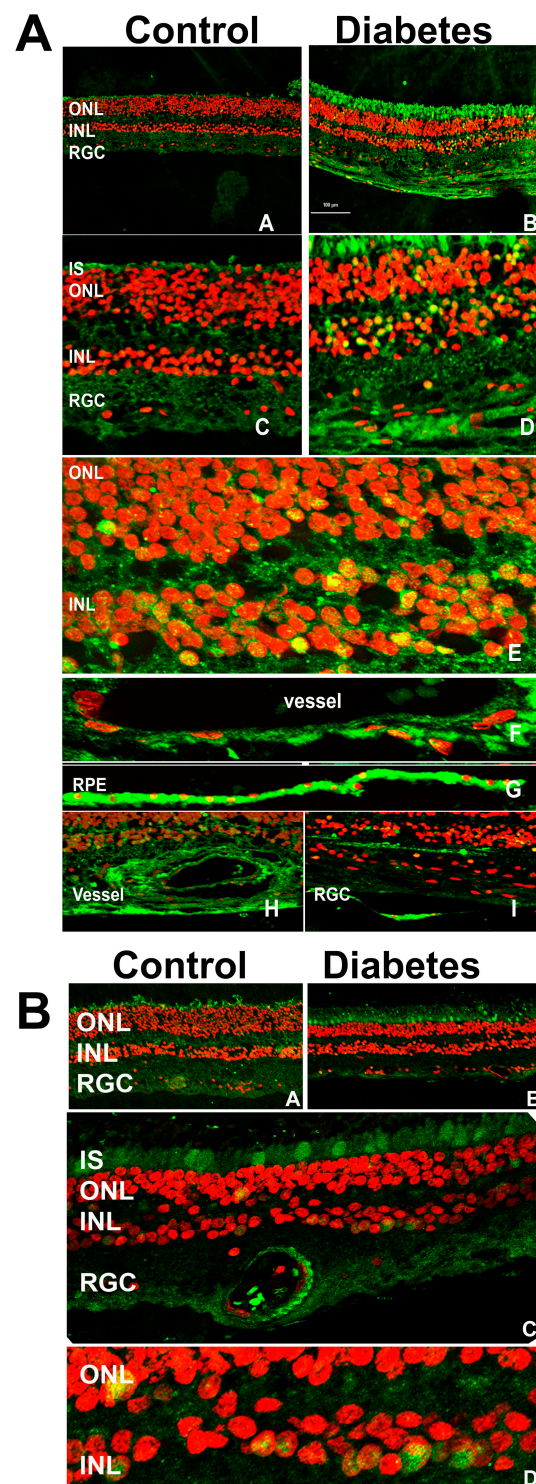


**Figure 1.** The immunohistochemical analysis of human control and diabetic retinas. (A) The retinas were subjected to treatment with anti-ChREBP antibody. The ChREBP immunoreactivity in human control (A,C) and diabetic (B,D) retinas. In the diabetic retina, robust staining of ChREBP (green) was detected in the photoreceptors, the cells of the INL (E), endothelial cells (F,H), retinal pigment epithelial cells (G), and retinal ganglion cells (I). The co-localization of ChREBP in the nuclei (red) of retinal cells is indicated in yellow. (B) The MondoA immunoreactivity in human control (A) and diabetic (B) retinas is shown in green. In the diabetic retina, robust staining was detected in the cones (C) and the cells of the INL (C). The localization of MondoA in the nuclei is shown in yellow (D).

Immunohistochemical analysis revealed extensive ChREBP expression across the retina (Figure 1A), with a notably stronger signal in the diabetic retinas compared to

the controls. Specifically, ChREBP was observed in photoreceptors, including the outer nuclear layer (ONL) and inner segments (IS) of photoreceptors, as well as in the inner nuclear layer (INL), where it demonstrated strong immunoreactivity. A key observation was the subcellular localization of ChREBP. In diabetic retinas, ChREBP was frequently detected in the nuclei, in contrast with the control retinas, where nuclear localization was significantly less pronounced. Additionally, ChREBP expression was detected in both retinal epithelial (RPE) cells (Figure 1A sub-panel G) and endothelial (HREC) cells of blood vessels (Figure 1A sub-panels F,H). These findings suggest that ChREBP is broadly expressed in the neuronal, epithelial, and endothelial cells of the retina. Moreover, its expression is enhanced in diabetic conditions, where it also shows increased nuclear translocation, indicating a potential role in mediating diabetes-induced retinal changes. Meanwhile, we observed that the expression profile of MondoA differed from that of ChREBP. MondoA expression was more prominent in cone photoreceptors than in rods. Like ChREBP, MondoA immunoreactivity was also detected in individual nuclei within the ONL and the INL.

In mouse diabetic retinas, RNAscope analysis showed elevated ChREBP mRNA levels compared to the controls (Figure 2A).

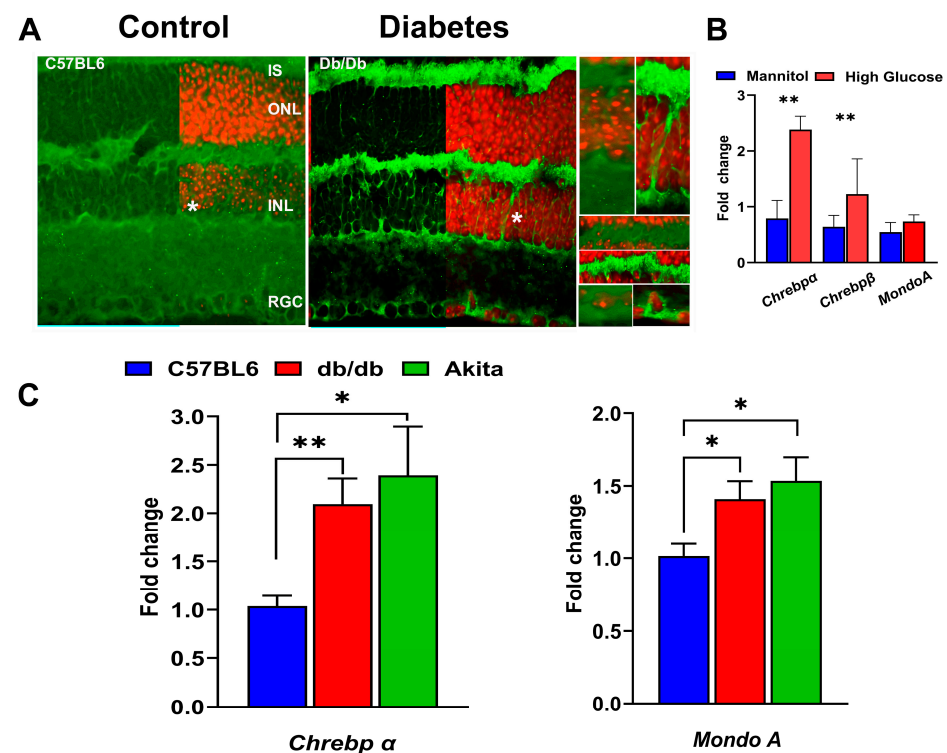


**Figure 2.** Expression of Mondo family proteins in hyperglycemic mouse retinas. (A) The RNAscope technique revealed enhanced ChREBP mRNA expression (green) in 12-week-old db/db retinas. The retinal ganglion cells (RGCs), Müller cells (highlighted in right inserts), and photoreceptors are responsive to hyperglycemia, showing increased ChREBP expression. (B) Mouse retinal explants were cultured in a medium supplemented with either high glucose or an equimolar concentration of mannitol (control) for 24 h. High-glucose, but not high-mannitol, culture conditions resulted in significant increases in both Chrebpα and Chrebpβ mRNAs, indicating that high glucose stimulates ChREBP expression ex vivo. (C) To confirm the ex vivo findings, diabetic retinas were isolated for qRT-PCR analysis to evaluate ChREBP and MondoA gene expression. The qRT-PCR results show that retinas from 12-week-old db/db and Akita mice exhibit increased expression of both Chrebp and MondoA mRNAs. Statistical significance is indicated as \*  $p < 0.05$  and \*\*  $p < 0.01$  ( $n = 4$  per group).

In 12-week-old db/db mice, ChREBP mRNA was detected in photoreceptors, Müller cells, and cells in the INL and retinal ganglion cells (RGCs). Furthermore, to assess whether

diabetic conditions stimulated ChREBP expression in the retina, retinal explants were exposed to high-glucose media. Real-time PCR analysis revealed marked upregulation of both ChREBP $\alpha$  and  $\beta$  isoforms due to high-glucose culture conditions (Figure 2B). However, MondoA expression showed no significant response to this treatment (Figure 2B). In contrast, in vivo, both the db/db and Akita mice retinas manifested elevated expression of ChREBP and MondoA mRNA compared to wild-type retinas (Figure 2C), although the increase in ChREBP expression in both diabetic retinas was more pronounced compared to MondoA expression. Altogether, the presented results demonstrate that both Mondo family proteins are expressed in the neuronal retinas of humans and mice, with some differences in the distribution of immunoreactivity between rods and cones. Hyperglycemic conditions further stimulate the expression of ChREBP and MondoA in the retinas.

### 3.2. Overexpression of ChREBP in Photoreceptors Results in Diminished Scotopic ERG Responses

To further investigate the role of ChREBP in rod photoreceptors and mimic the increased ChREBP expression observed in diabetic retinas, we generated mice with constitutively active (ca) ChREBP expression in the rods (Figure 3A).

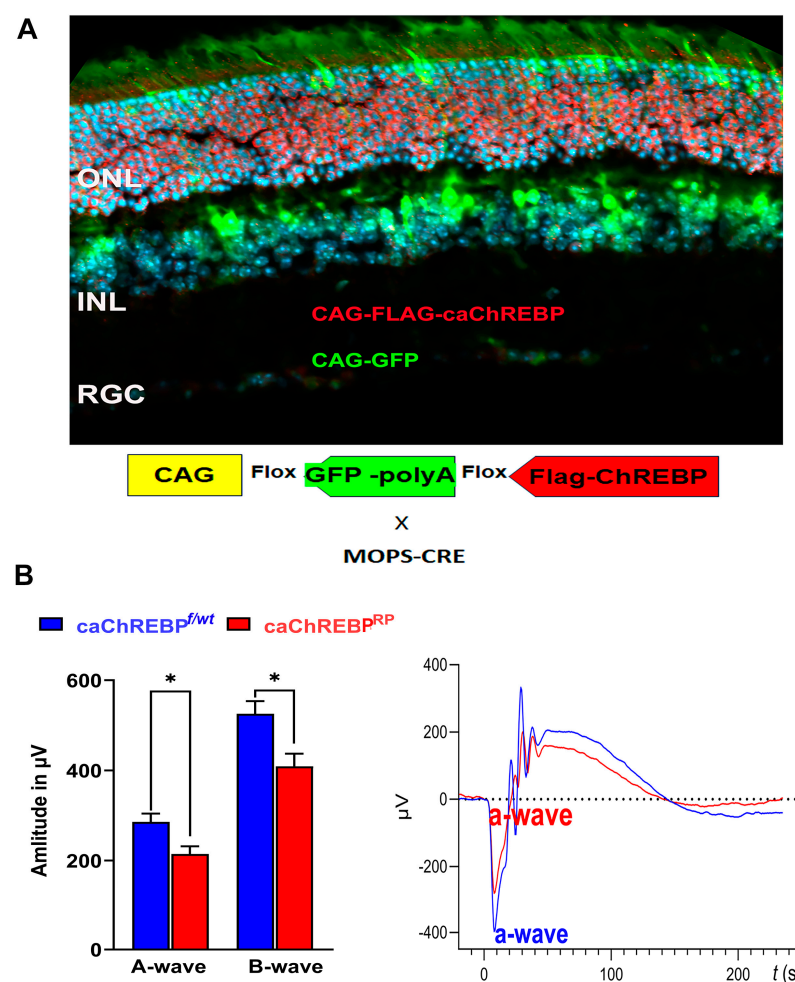


**Figure 3.** Transgenic expression of constitutively active ChREBP in mouse rods leads to vision loss. (A) i-Cre-mediated recombination in rod photoreceptors of caChREBP<sup>RP</sup> transgenic mice resulted in deletion of eGFP and expression of FLAG-tagged caChREBP, detected by anti-FLAG antibody, shown in red. Nuclei are shown in blue. (B) Expression of caChREBP in rod photoreceptors leads to reduction in scotopic a- and b-wave amplitudes in caChREBP<sup>RP</sup> versus control (eGFP<sup>flox/wt</sup>-caChREBP or CgChREBP<sup>f/wt</sup>) mice at postnatal day 35. Representative waveforms are shown on right. \*  $p < 0.05$ ,  $n = 3$ –6 per group.

eGFP<sup>flox</sup>/wt-caChREBP mice have been described previously and, in the absence of Cre recombinase, ubiquitously express the enhanced green fluorescent protein (eGFP), the genetic sequence for which is located between two loxP sites and which is immediately upstream of a sequence for N-terminal FLAG-tagged caChREBP [11]. Excision of the eGFP sequence and subsequent expression of FLAG-tagged caChREBP occurs following Cre recombination. I-Cre mice express Cre recombinase under the control of the short mouse rod opsin (MOPS) promoter, ensuring caChREBP expression, specifically in rod photoreceptors (RPs). As expected, the caChREBP<sup>RP</sup> retinas exhibited GFP expression in cells lacking Cre recombination (such as cone photoreceptors or cells of the INL), while the FLAG-tagged caChREBP, detected with anti-FLAG antibody and shown in red, was observed in rod photoreceptors.

In the p35 caChREBP<sup>RP</sup> mice, ERG analysis revealed a reduction in scotopic a- and b-wave amplitudes compared to eGFP<sup>flox</sup>/wt-caChREBP (ChREBP<sup>f</sup>/wt) (Figure 3B). The ERG amplitudes recorded with other intensities are shown in Figure S1. No significant loss of photopic ERG amplitude was observed in caChREBP<sup>RP</sup> mice at this point. These data suggest that the ChREBP upregulation observed in diabetic retinas could contribute to the loss of retinal function in diabetic mice. Therefore, we became interested in ChREBP-mediated cellular signaling and performed a study of global proteomics with caChREBP<sup>RP</sup> retinas.

### 3.3. Overexpression of ChREBP in Photoreceptors Alters Retinal Proteomics

The constitutive expression of ChREBP in rod photoreceptors of caChREBP<sup>RP</sup> mice led to substantial changes in the protein landscape within the retina, affecting several key metabolic, structural, and signaling pathways. Over 40 proteins were differentially expressed ( $p < 0.05$ ) in the caChREBP retinas, both upregulated and downregulated. A heat map of the top-modified proteins is shown in Figure 4A.

The list of upregulated proteins included hexokinase 2, glucosidase 2, splicing factor 3B, and NADPH-cytochrome P450 reductase. The list of downregulated proteins contained tight junction protein zonula occludens 1 (ZO1), PDE6 $\alpha$ , GNAT2, and the succinate-semialdehyde dehydrogenase mitochondrial enzyme (Figure S2). Figure S3 presents an analysis of the ingenuity pathways modified by the upstream regulator ChREBP (MLXIPL), which had the highest Z-score activation as an upstream regulator in this experiment.

Given that following G6P allosteric binding, ChREBP translocates to the nucleus and forms a complex with MLX to bind the carbohydrate response element (ChoRE) in the target gene promoters, we examined its downstream signaling, as this activation is central to ChREBP's role in metabolic gene regulation, especially in conditions of high glucose. TXNIP is a well-known ChREBP target gene containing the ChoRE element [3]. This protein is also significantly implicated in DR, as it inhibits a major antioxidant protein, thioredoxin. Elevated TXNIP in diabetic retinas is thought to contribute to cellular stress and disease progression. In our study, TXNIP expression increased by about 50% in caChREBP<sup>RP</sup> retinas, consistent with ChREBP's role in promoting TXNIP-induced cell death (Figure 4B) [17].

Using ShinyGO 8.0, we then analyzed a list of downregulated KEGG signaling pathways in caChREBP<sup>RP</sup> retinas (Figure 4C). This analysis revealed significant downregulation in pathways related to histidine, alanine, arginine, and purine metabolism. Consistent with our previous findings on retinal physiology, the phototransduction pathway was identified as one of the primary downregulated KEGG pathways, indicating a potential decline in retinal function. These findings indicate that the upregulation of proteins involved in glucose metabolism, glycoprotein biosynthesis, and oxidative stress, together with protein changes affecting the visual cycle, mitochondrial energy, and amino acid metabolism, underscores ChREBP's influence on retinal metabolism and structure.



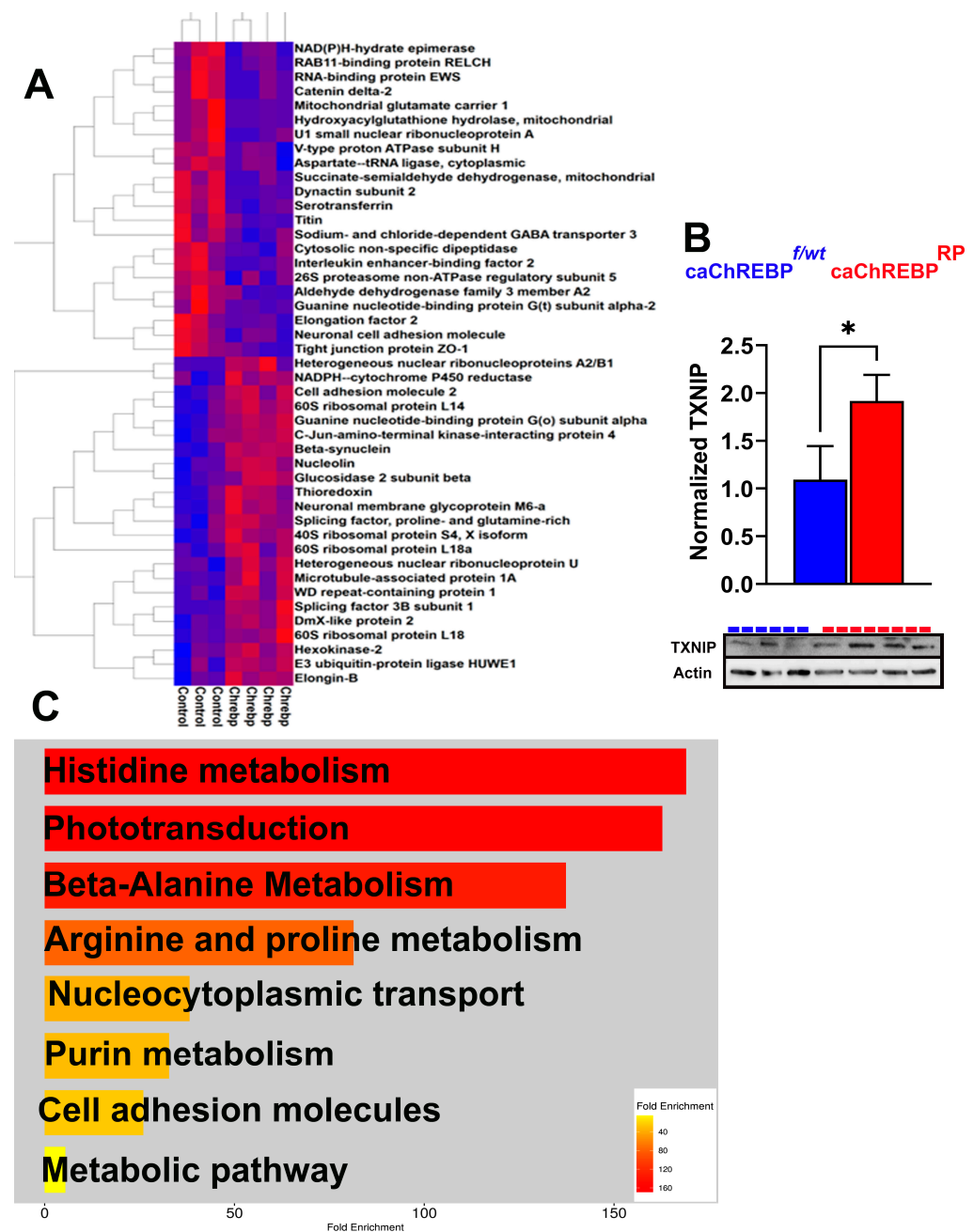


**Figure 4.** Increased ChREBP activity in rods alters retinal proteomics and KEGG signaling in caChREBP<sup>RP</sup> mice. (A) Heatmap showing major altered proteins in caChREBP<sup>RP</sup> compared with eGFP<sup>fllox/wt</sup>-caChREBP control (Control) retinas ( $n = 3\text{--}4$  per group), highlighting significant changes in retinal protein expression. (B) Expression of constitutively active ChREBP (caChREBP) in rods leads to increase in TXNIP levels at postnatal day 35 (P35). Statistical significance is indicated by \*  $p < 0.05$ , with  $n = 3\text{--}4$  per group. (C) Major downregulated KEGG signaling pathways in caChREBP-expressing retinas are identified, showing significant pathway alterations due to sustained ChREBP activity in rods.

### 3.4. Overexpression of Human ChREBP in ARPE-19 Cells Causes Metabolic Reprogramming and Alters Cellular Signaling

Hyperglycemia also affects RPE cell health [18–20]. Under diabetic conditions, hyperglycemia induces metabolic reprogramming in the RPE cells, leading to a glycolytic shift due to trapped glucose [20]. This glucose may contribute not only to aerobic glycolysis but also to the activation of ChREBP [20]. Therefore, knowing that ChREBP is expressed in RPE [15], we next infected the ARPE-19 cells with lentiviral particles expressing ChREBP



for 48 h. After harvesting, cells were subjected to the preparation of protein extracts and global proteome analysis by LC-MS. Overall, 36 proteins were differentially expressed in the treated RPE group, and ChREBP was one of them (Figure S4). Figure 5 depicts a heat map of the top differentially expressed proteins with  $p < 0.05$ . This map indicates that hexokinase-1, LAMP1, LAMP2, and mitochondrial Acetyl-coA acyltransferase were upregulated, while the large ribosomal uL23 and 26 proteasome non-ATPase regulatory subunits were downregulated.

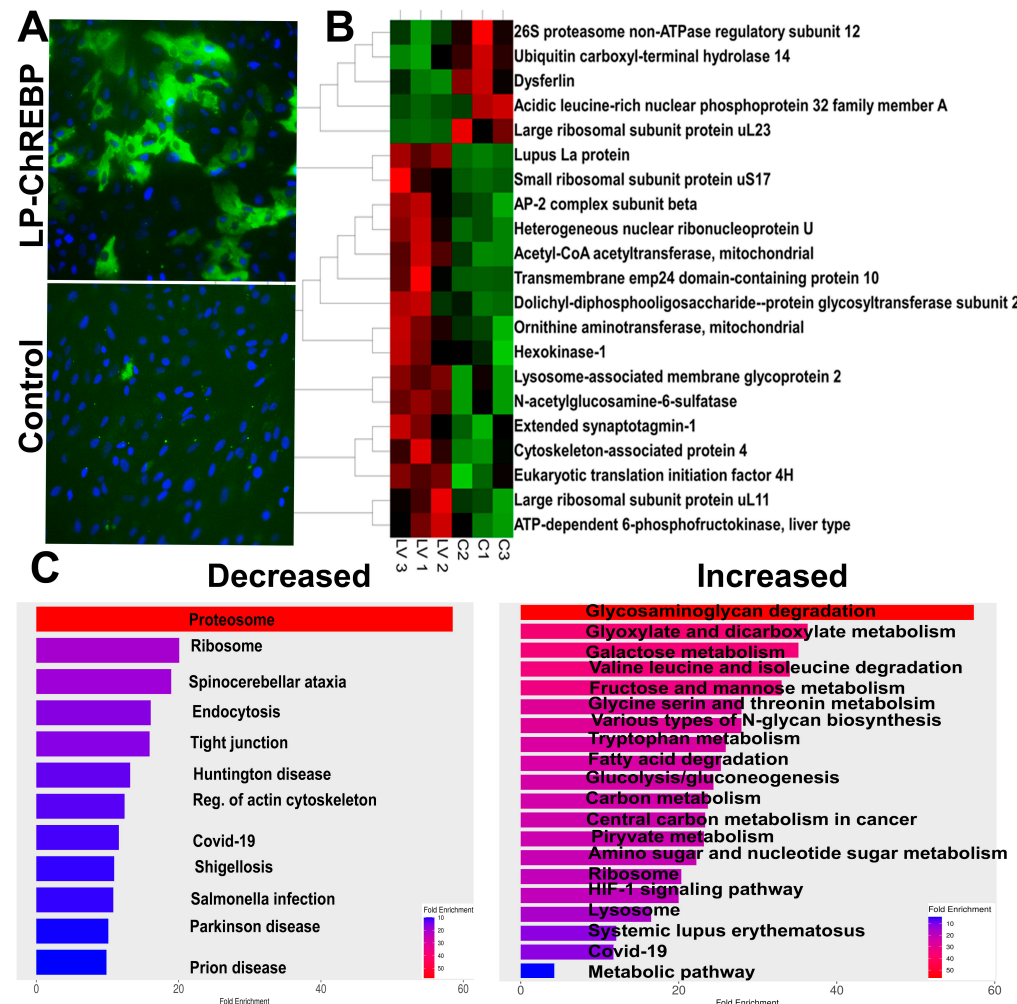


**Figure 5.** Overexpression of ChREBP in human ARPE-19 cells. (A) The images of ARPE-19 cells overexpressing human ChREBP and control cells treated with the empty virus. The direct fluorescence emitted by GFP indicates successful infection and ChREBP expression. (B) The heatmap displays the major altered proteins in ARPE-19 cells with sustained ChREBP expression ( $n = 3-4$  per group), highlighting significant protein expression changes due to ChREBP overexpression. (C) The results from the proteomic analysis were analyzed using the Shiny GO program to generate diagrams of altered KEGG pathways. Both decreased and increased pathways are shown, reflecting the impact of sustained ChREBP expression on cellular signaling networks in ARPE-19 cells.

The analysis of KEGG signaling pathways indicates that glyoxylate and dicarboxylate metabolism, sugar (including galactose, fructose, and mannose) metabolism, and glycolysis itself increased in ARPE-19 cells overexpressing ChREBP. These changes aligned with the activation of the lysosome pathway. Meanwhile, as observed for the retina with ChREBP overexpression in photoreceptors, tight junction signaling was diminished following treatment, along with a reduction in proteasome signaling. Further analysis of altered molecular function in treated cells demonstrated an increase in acetyl-CoA acetyltransferase activity, while TORC2 complex-binding activity was downregulated (Figure 6).

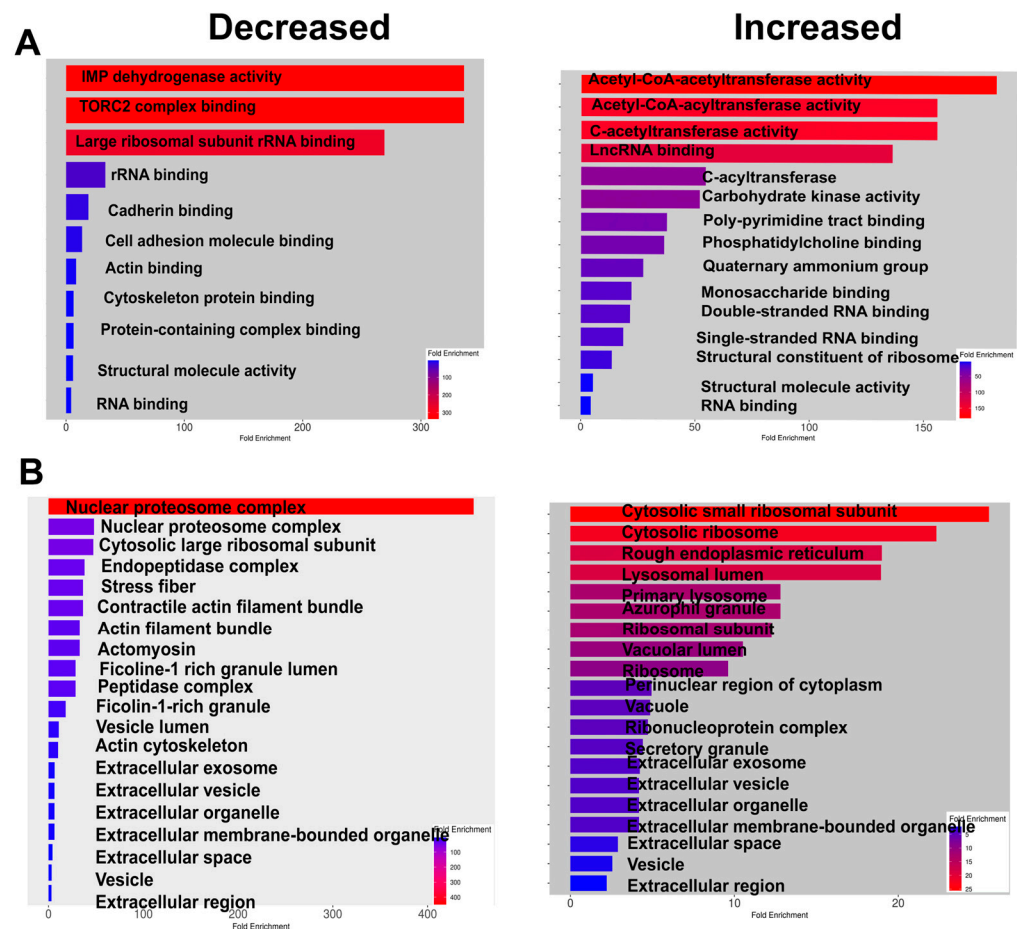


**Figure 6.** ChREBP overexpression alters molecular function and affects cellular components of human ARPE-19 cells. **(A)** The molecular functions that are decreased or increased due to ChREBP overexpression in ARPE-19 cells are shown, highlighting the functional alterations induced by sustained ChREBP expression. **(B)** The cellular components affected by ChREBP expression in ARPE-19 cells are presented, demonstrating how ChREBP overexpression leads to changes in the cellular architecture and composition ( $n = 3\text{--}4$  per group).

Consistent with observations in the with ChREBP<sup>RP</sup> retina, the cell adhesion complex was reduced in response to ChREBP overexpression, including cadherin binding. The function of major cellular components, such as the nuclear proteasome and proteasome complexes, declined. In addition, ChREBP overexpression enhanced the formation of a cytosolic small ribosomal complex and lysosomes (Figure 6).

#### 4. Discussion

In this study, we sought to better understand the expression patterns of ChREBP and MondoA, with the aim of clarifying a potential role of ChREBP in the pathogenesis of DR. The role of the MondoA family of proteins has been studied in various metabolic diseases, including cancer and diabetes. With few exceptions in the literature highlighting the role of ChREBP in endothelial and RPE cells, no studies have been conducted on healthy or diseased retinal tissues, indicating a gap in our knowledge of DR pathogenesis [14,15]. To the best of our knowledge, this is the first study to demonstrate the expression of ChREBP and MondoA in human retinas. Furthermore, we also investigated ChREBP and MondoA expression during the progression of DR and found that both mRNAs were elevated in T1D and T2D mouse retinas. Using transgenic mice, we replicated the increased ChREBP expression in retinas observed under diabetic conditions in the retinas and found that ChREBP overexpression in rod photoreceptors appears to be harmful,

leading to retinal functional loss associated with the alteration of metabolic pathways. Finally, both photoreceptor cells and RPE cells overexpressing ChREBP manifest metabolic reprogramming and compromised molecular function, highlighting the potential role of ChREBP in diabetic RPE.

The retina is a highly metabolic tissue, making it particularly vulnerable to metabolic disturbances, such as DR. Indeed, the retinal glucose level rises upon sustained hyperglycemia, controlling the expression of glucose-regulated proteins and leading to unscheduled glycolysis and activation of the polyol pathway, hexosamine, and the PKC and AGE pathways [20–22]. Both glucose-sensing ChREBP and MondoA proteins are expressed in the retina, although their expression patterns differ. ChREBP is expressed in photoreceptors, endothelial cells (vessels), retinal epithelial cells (RPE), and other neuronal cells (INL). In contrast, MondoA expression appears to be more robust in cone photoreceptors. These results are in agreement with the depository database “The human protein atlas,” suggesting its expression in cones is the highest in the entire human body (<https://www.proteinatlas.org/ENSG00000175727-MLXIP/single+cell>, accessed on 8 October 2024). In addition, we performed a search of single-cell RNA-seq databases to identify retinal cell populations expressing MLXIPL (ChREBP) and MLXIP (MondoA). Figures S5 and S6 present the results obtained from human and mouse retinas, respectively. Notably, both databases revealed widespread expression of these genes in retinal cells, with more robust expression of MLXIP (MondoA) observed in cones compared to rods.

Diabetes induces an increase in ChREBP and MondoA mRNA levels in the retina. High glucose regulates the expression of both proteins. In cases of hyperglycemia, following G6P-promoted allosteric conformational changes, both MFPs translocate to the nucleus and independently bind the MLX transcription factor, activating the expression of genes via the ChoRE element within the promoters of target genes, such as TXNIP. In line with this, we observed strong ChREBP immunoreactivity in the nuclei of photoreceptors and other neurons whose nuclei could be found in the retina’s inner nuclear layer upon hyperglycemia. Furthermore, overexpression of ChREBP in photoreceptors leads to an increase in TXNIP, suggesting a mechanism through which DR directly affects cell viability.

Transgenic caChREBP overexpression results in a decline in retinal function. Both a- and b-wave scotopic ERG amplitudes are diminished. Ongoing research on retinal dysfunction has reported reduced cone sensitivity [23], delayed activation of cone phototransduction cascade [24], selective loss of S cones [25,26], glial abnormalities, and thinning of both the nerve fiber and the RGC layer in individuals with DR [27–29] and animal models of DR [21,30–32]. Our data point to a mechanism through which diabetes, associated with sustained ChREBP activity and increased expression of ChoRE element-containing target genes such as TXNIP in the retina, may result in loss of vision and an altered proteomic landscape of the diabetic retina.

Indeed, ChREBP overexpression resulted in an altered protein profile in p35 caChREBP<sup>RP</sup> retinas. These changes were mostly associated with elevated glucose metabolism. For example, hexokinase-2 initiates glycolysis. Glucosidase 2, a key enzyme for glycoprotein biosynthesis, processes glycoproteins. Splicing factor 3 is a part of the splicing machinery complex and regulates gene expression. Meanwhile, the caChREBP<sup>RP</sup> retina manifests compromised cell-to-cell adhesion and blood–retinal barrier integrity, as ZO1 protein levels decline. In line with this, a reduction in proteins responsible for mitochondrial energy metabolism, such as the glutamate carrier and sodium- and chloride-dependent GABA transporter 3, was observed. The compromised expression of these proteins, along with reduced rod-specific PDE6 $\alpha$ , is most likely associated with a decline in phototransduction, as mice deficient in PDE6 $\alpha$  manifest dramatic vision loss [33].

Another change observed in the diabetic retina included compromised histidine and alanine metabolism. In addition to their roles as amino acids essential for protein synthesis, histidine can be converted to histamine, a neurotransmitter and immune modulator whose deficiency may contribute to neurological problems. A lack of alanine in the retina may further disrupt cellular function too, as alanine plays a critical role in energy metabolism, serving as a key substrate in the glucose–alanine cycle. Disruption of this cycle could lead to impaired energy balance and the accumulation of toxic byproducts, potentially contributing to retinal dysfunction. In line with these findings, ChREBP overexpression in RPE cells alters cellular metabolism as well. Indeed, RPE cells have several unique metabolic features. For example, they manifest the high amount of lipid processing necessary for the visual cycle as they regenerate visual pigments. RPE cells phagocytose photoreceptor outer segments and routinely digest photoreceptor outer segments, a highly demanding process that involves extensive lipid and protein degradation. RPE cells contain robust antioxidant systems, including elevated levels of glutathione, superoxide dismutase, and catalase, because of their adaptation to high metabolic activity, constant light exposure, and oxygen consumption. Finally, RPE cells rely on both oxidative phosphorylation and glycolysis to meet their energy demands, and their metabolism strongly depends on lactate. Therefore, the observed metabolic reprogramming disturbs homeostasis.

Glyoxylate has been proposed as a new metabolite marker of T2D [34]. A significant increase in glyoxylate levels was observed in the plasma of db/db mice, and detected in the plasma of humans three years prior to the diagnosis of diabetes. Moreover, it has been proposed that elevated glyoxylate may contribute to an increase in advanced glycation end products (AGEs) [34]. RPE cells overexpressing ChREBP manifested an increase in glyoxylate and dicarboxylate metabolism, supporting that sustained elevation of ChREBP during diabetes may enhance the conversion of enhanced glyoxylate to advanced glycation end products. In support of this hypothesis, the proteasome system is compromised in treated ARPE-19 cells, which could create conditions favorable for AGE production [35].

The decline in the function of the nuclear proteasome and proteasome complexes could indicate impaired protein degradation, which may lead to the accumulation of damaged or unnecessary proteins. Meanwhile, ChREBP overexpression enhances lysosomal activity, to manage excess generated proteins or to compensate for the reduced protein degradation capacity under conditions influenced by ChREBP overexpression. In agreement with this, the LAMP1 and LAMP2 proteins, as well as the HIF-1 signaling for which lysosomes act as a degradation organelle [36], were upregulated. Moreover, the highest increase in glycosaminoglycan degradation supports this hypothesis as well. Glycosaminoglycans, long chains of negatively charged polysaccharides, are degraded by lysosomes [37].

Overall, our findings point to the critical need for a thorough examination of the role of glucose-activated proteins in DR.

## 5. Conclusions

In conclusion, this study is the first to demonstrate that Mondo family proteins, ChREBP and MondoA, are expressed throughout the retina and upregulated in humans with diabetic retinopathy and in murine models. This overexpression reprograms cellular metabolism, leading to vision loss. Therefore, these findings highlight a pivotal role for elevated ChREBP in DR and emphasize the therapeutic potential of targeting ChREBP and MondoA, paving the way for further research into novel treatments.

**Supplementary Materials:** The following supporting information can be downloaded at: <https://www.mdpi.com/article/10.3390/cells14020107/s1>, Figure S1: ERG analysis conducted with caChREBP<sup>RP</sup> mice at −20 dB, 0 dB, and 10 dB. Figure S2: Quantitative spectrum counts for the proteomic analysis of caChREBP<sup>RP</sup> retinas. Figure S3: Ingenuity pathways significantly changed

by ChREBP overexpression in rods of caChREBP<sup>RP</sup> mice. Upstream regulator MLXIPL/ChREBP had the highest positive Z score for the activating transcriptional program. Figure S4: Quantitative spectrum counts for the proteomic analysis of the ARPE-19 cells overexpressing ChREBP. Figure S5: A violin plot was generated using single-cell RNA-seq (scRNA-seq) data from the human retina, retinal pigment epithelium (RPE), and choroid. Figure S6: A violin plot was generated using single-cell RNA-seq (scRNA-seq) data from the mouse retina.

**Author Contributions:** Conceptualization, M.G.; methodology, M.G., C.R.S. and A.Z.; software, J.M. and C.R.S.; validation, C.R.S. and O.G.; formal analysis, C.R.S. and M.G.; resources M.G. and A.M.N.-A.; data curation, M.G., C.R.S., A.Z. and O.G.; writing—original draft preparation, M.G. and C.R.S.; writing—review and editing, M.B.G., C.R.S. and A.M.N.-A.; visualization, M.G., O.G., C.R.S., A.Z. and J.M.; supervision, M.G.; project administration, M.G. All authors have read and agreed to the published version of the manuscript.

**Funding:** This study was supported by the National Eye Institute, grant number R01 EY035539 and R01 EY 033620.

**Institutional Review Board Statement:** The animal study protocol was approved by the University of Alabama at Birmingham’s institutional animal care and use committee (protocol no. 22104).

**Informed Consent Statement:** Not applicable.

**Data Availability Statement:** The research data are available upon request. The raw data are also available as Supplementary Materials.

**Acknowledgments:** The normal human and diabetic retinas were a gift from Mohamed Al-Shabrawey at Oakland University.

**Conflicts of Interest:** The authors declare no conflicts of interest.

## Abbreviations

MFPs	Mondo family proteins
ChREB or MLXIPL	Carbohydrate response element-binding protein
MLXIP	MondoA protein
caChREBP	Constitutively active ChREBP
G6P	Glucose-6-phosphate
caChREBP <sup>RP</sup>	Rod photoreceptor-specific caChREBP
MLX	Max-like protein X
TXNIP	Thioredoxin-interacting protein
ARRDC4	Arrestin Domain-Containing Protein 4
RPE cells	Retinal epithelial cells
HREC	Retinal endothelial cells
KEGG	Kyoto Encyclopedia of Genes and Genomes
NADPH	Reduced nicotinamide adenine dinucleotide phosphate
PDE6 $\alpha$	Phosphodiesterase $\alpha$ subunit
	Transducin GNAT2
LAMP1/20	Lysosome-associated membrane protein 1/2
TORC2	Target Of Rapamycin Complex 2
AGE	Advanced glycation end product
T2D	Type 2 diabetes

## References

1. Billin, A.N.; Eilers, A.L.; Coulter, K.L.; Logan, J.S.; Ayer, D.E. MondoA, a novel basic helix-loop-helix-leucine zipper transcriptional activator that constitutes a positive branch of a max-like network. *Mol. Cell Biol.* **2000**, *20*, 8845–8854. [[CrossRef](#)] [[PubMed](#)]
2. Stoeckman, A.K.; Ma, L.; Towle, H.C. Mlx is the functional heteromeric partner of the carbohydrate response element-binding protein in glucose regulation of lipogenic enzyme genes. *J. Biol. Chem.* **2004**, *279*, 15662–15669. [[CrossRef](#)] [[PubMed](#)]



3. Nieborak, A.; Lukauskas, S.; Capellades, J.; Heyn, P.; Santos, G.S.; Motzler, K.; Zeigerer, A.; Bester, R.; Protzer, U.; Schelter, F.; et al. Depletion of pyruvate kinase (PK) activity causes glycolytic intermediate imbalances and reveals a PK-TXNIP regulatory axis. *Mol. Metab.* **2023**, *74*, 101748. [\[CrossRef\]](#) [\[PubMed\]](#)
4. Yu, F.X.; Luo, Y. Tandem ChoRE and CCAAT motifs and associated factors regulate Txnip expression in response to glucose or adenosine-containing molecules. *PLoS ONE* **2009**, *4*, e8397. [\[CrossRef\]](#)
5. Ahn, B.; Wan, S.; Jaiswal, N.; Vega, R.B.; Ayer, D.E.; Titchenell, P.M.; Han, X.; Won, K.J.; Kelly, D.P. MondoA drives muscle lipid accumulation and insulin resistance. *JCI Insight* **2019**, *4*, e129119. [\[CrossRef\]](#)
6. Ahn, B.; Soundarapandian, M.M.; Sessions, H.; Peddibhotla, S.; Roth, G.P.; Li, J.L.; Sugarman, E.; Koo, A.; Malany, S.; Wang, M.; et al. MondoA coordinately regulates skeletal myocyte lipid homeostasis and insulin signaling. *J. Clin. Investig.* **2016**, *126*, 3567–3579. [\[CrossRef\]](#)
7. Iizuka, K.; Takao, K.; Kato, T.; Horikawa, Y.; Takeda, J. ChREBP Reciprocally Regulates Liver and Plasma Triacylglycerol Levels in Different Manners. *Nutrients* **2018**, *10*, 1699. [\[CrossRef\]](#)
8. Linden, A.G.; Li, S.; Choi, H.Y.; Fang, F.; Fukasawa, M.; Uyeda, K.; Hammer, R.E.; Horton, J.D.; Engelking, L.J.; Liang, G. Interplay between ChREBP and SREBP-1c coordinates postprandial glycolysis and lipogenesis in livers of mice. *J. Lipid Res.* **2018**, *59*, 475–487. [\[CrossRef\]](#)
9. Ke, H.; Luan, Y.; Wu, S.; Zhu, Y.; Tong, X. The Role of Mondo Family Transcription Factors in Nutrient-Sensing and Obesity. *Front. Endocrinol.* **2021**, *12*, 653972. [\[CrossRef\]](#)
10. Benhamed, F.; Denechaud, P.D.; Lemoine, M.; Robichon, C.; Moldes, M.; Bertrand-Michel, J.; Ratzliff, V.; Serfaty, L.; Housset, C.; Capeau, J.; et al. The lipogenic transcription factor ChREBP dissociates hepatic steatosis from insulin resistance in mice and humans. *J. Clin. Investig.* **2012**, *122*, 2176–2194. [\[CrossRef\]](#)
11. Nuotio-Antar, A.M.; Pongvarin, N.; Li, M.; Schupp, M.; Mohammad, M.; Gerard, S.; Zou, F.; Chan, L. FABP4-Cre Mediated Expression of Constitutively Active ChREBP Protects Against Obesity, Fatty Liver, and Insulin Resistance. *Endocrinology* **2015**, *156*, 4020–4032. [\[CrossRef\]](#)
12. Herman, M.A.; Peroni, O.D.; Villoria, J.; Schon, M.R.; Abumrad, N.A.; Bluher, M.; Klein, S.; Kahn, B.B. A novel ChREBP isoform in adipose tissue regulates systemic glucose metabolism. *Nature* **2012**, *484*, 333–338. [\[CrossRef\]](#) [\[PubMed\]](#)
13. Li, M.V.; Chang, B.; Imamura, M.; Pongvarin, N.; Chan, L. Glucose-dependent transcriptional regulation by an evolutionarily conserved glucose-sensing module. *Diabetes* **2006**, *55*, 1179–1189. [\[CrossRef\]](#) [\[PubMed\]](#)
14. Sui, Y.; Du, C.; Wang, M.; Liu, X.; Chai, Q.; Liang, S.; Ma, J.; Duan, J. Knockdown of ChREBP ameliorates retinal microvascular endothelial cell injury and angiogenic responses in diabetic retinopathy. *Biochem. Biophys. Res. Commun.* **2024**, *694*, 149389. [\[CrossRef\]](#) [\[PubMed\]](#)
15. Chang, M.L.; Chiu, C.J.; Shang, F.; Taylor, A. High glucose activates ChREBP-mediated HIF-1 $\alpha$  and VEGF expression in human RPE cells under normoxia. *Adv. Exp. Med. Biol.* **2014**, *801*, 609–621. [\[CrossRef\]](#)
16. Zhylkibayev, A.; Ung, T.T.; Mobley, J.; Athar, M.; Gorbatyuk, M. The Involvement of Unfolded Protein Response in the Mechanism of Nitrogen Mustard-Induced Ocular Toxicity. *J. Pharmacol. Exp. Ther.* **2024**, *388*, 518–525. [\[CrossRef\]](#)
17. Singh, L.P. Thioredoxin Interacting Protein (TXNIP) and Pathogenesis of Diabetic Retinopathy. *J. Clin. Exp. Ophthalmol.* **2013**, *4*, 10. [\[CrossRef\]](#)
18. Tonade, D.; Kern, T.S. Photoreceptor cells and RPE contribute to the development of diabetic retinopathy. *Prog. Retin. Eye Res.* **2021**, *83*, 100919. [\[CrossRef\]](#)
19. Maugeri, G.; Bucolo, C.; Drago, F.; Rossi, S.; Di Rosa, M.; Imbesi, R.; D'Agata, V.; Giunta, S. Attenuation of High Glucose-Induced Damage in RPE Cells through p38 MAPK Signaling Pathway Inhibition. *Front. Pharmacol.* **2021**, *12*, 684680. [\[CrossRef\]](#)
20. Yumnamcha, T.; Guerra, M.; Singh, L.P.; Ibrahim, A.S. Metabolic Dysregulation and Neurovascular Dysfunction in Diabetic Retinopathy. *Antioxidants* **2020**, *9*, 1244. [\[CrossRef\]](#)
21. Pitale, P.M.; Saltykova, I.V.; Adu-Agyeiwaah, Y.; Calzi, S.L.; Satoh, T.; Akira, S.; Gorbatyuk, O.; Boulton, M.E.; Pardue, M.T.; Garvey, W.T.; et al. Tribbles Homolog 3 Mediates the Development and Progression of Diabetic Retinopathy. *Diabetes* **2021**, *70*, 1738–1753. [\[CrossRef\]](#) [\[PubMed\]](#)
22. Holoman, N.C.; Aiello, J.J.; Trobenter, T.D.; Tarchick, M.J.; Kozlowski, M.R.; Makowski, E.R.; De Vivo, D.C.; Singh, C.; Sears, J.E.; Samuels, I.S. Reduction of Glut1 in the Neural Retina But Not the RPE Alleviates Polyol Accumulation and Normalizes Early Characteristics of Diabetic Retinopathy. *J. Neurosci.* **2021**, *41*, 3275–3299. [\[CrossRef\]](#) [\[PubMed\]](#)
23. Weiner, A.; Christopoulos, V.A.; Gussler, C.H.; Adams, D.H.; Kaufman, S.R.; Kohn, H.D.; Weidenthal, D.T. Foveal cone function in nonproliferative diabetic retinopathy and macular edema. *Investig. Ophthalmol. Vis. Sci.* **1997**, *38*, 1443–1449.
24. McAnany, J.J.; Park, J.C. Cone Photoreceptor Dysfunction in Early-Stage Diabetic Retinopathy: Association Between the Activation Phase of Cone Phototransduction and the Flicker Electroretinogram. *Investig. Ophthalmol. Vis. Sci.* **2019**, *60*, 64–72. [\[CrossRef\]](#)
25. Cho, N.C.; Poulsen, G.L.; Ver Hoeve, J.N.; Nork, T.M. Selective loss of S-cones in diabetic retinopathy. *Arch. Ophthalmol.* **2000**, *118*, 1393–1400. [\[CrossRef\]](#)

26. Nomura, R.; Terasaki, H.; Hirose, H.; Miyake, Y. Blue-on-yellow perimetry to evaluate S cone sensitivity in diabetics. *Ophthalmic Res.* **2000**, *32*, 69–72. [[CrossRef](#)]
27. Verbraak, F.D. Neuroretinal degeneration in relation to vasculopathy in diabetes. *Diabetes* **2014**, *63*, 3590–3592. [[CrossRef](#)]
28. Verma, A.; Rani, P.K.; Raman, R.; Pal, S.S.; Laxmi, G.; Gupta, M.; Sahu, C.; Vaitheeswaran, K.; Sharma, T. Is neuronal dysfunction an early sign of diabetic retinopathy? Microperimetry and spectral domain optical coherence tomography (SD-OCT) study in individuals with diabetes, but no diabetic retinopathy. *Eye* **2009**, *23*, 1824–1830. [[CrossRef](#)]
29. Vujosevic, S.; Midena, E. Retinal layers changes in human preclinical and early clinical diabetic retinopathy support early retinal neuronal and Muller cells alterations. *J. Diabetes Res.* **2013**, *2013*, 905058. [[CrossRef](#)]
30. Gorbatyuk, O.S.; Pitale, P.M.; Saltykova, I.V.; Dorofeeva, I.B.; Zhylkibayev, A.A.; Athar, M.; Fuchs, P.A.; Samuels, B.C.; Gorbatyuk, M.S. A Novel Tree Shrew Model of Diabetic Retinopathy. *Front. Endocrinol.* **2021**, *12*, 799711. [[CrossRef](#)]
31. Hanaguri, J.; Yokota, H.; Watanabe, M.; Yamagami, S.; Kushiya, A.; Kuo, L.; Nagaoka, T. Retinal blood flow dysregulation precedes neural retinal dysfunction in type 2 diabetic mice. *Sci. Rep.* **2021**, *11*, 18401. [[CrossRef](#)] [[PubMed](#)]
32. Lam, C.H.; Zou, B.; Chan, H.H.; Tse, D.Y. Functional and structural changes in the neuroretina are accompanied by mitochondrial dysfunction in a type 2 diabetic mouse model. *Eye Vis.* **2023**, *10*, 37. [[CrossRef](#)] [[PubMed](#)]
33. Liu, Z.; Chen, S.; Davis, A.E.; Lo, C.H.; Wang, Q.; Li, T.; Ning, K.; Zhang, Q.; Zhao, J.; Wang, S.; et al. Efficient Rescue of Retinal Degeneration in Pde6a Mice by Engineered Base Editing and Prime Editing. *Adv. Sci.* **2024**, *11*, e2405628. [[CrossRef](#)] [[PubMed](#)]
34. Nikiforova, V.J.; Giesbertz, P.; Wiemer, J.; Bethan, B.; Looser, R.; Liebenberg, V.; Ruiz Noppinger, P.; Daniel, H.; Rein, D. Glyoxylate, a new marker metabolite of type 2 diabetes. *J. Diabetes Res.* **2014**, *2014*, 685204. [[CrossRef](#)] [[PubMed](#)]
35. Taylor, A.; Bejarano, E. Boosting proteolytic pathways as a treatment against glycation-derived damage in the brain? *Neural Regen. Res.* **2022**, *17*, 320–322. [[CrossRef](#)]
36. Hong, J.; Min, Y.; Wuest, T.; Lin, P.C. Vav1 is Essential for HIF-1alpha Activation via a Lysosomal VEGFR1-Mediated Degradation Mechanism in Endothelial Cells. *Cancers* **2020**, *12*, 1374. [[CrossRef](#)]
37. Fuller, M.; Meikle, P.J.; Hopwood, J.J. Glycosaminoglycan degradation fragments in mucopolysaccharidosis I. *Glycobiology* **2004**, *14*, 443–450. [[CrossRef](#)]

**Disclaimer/Publisher’s Note:** The statements, opinions and data contained in all publications are solely those of the individual author(s) and contributor(s) and not of MDPI and/or the editor(s). MDPI and/or the editor(s) disclaim responsibility for any injury to people or property resulting from any ideas, methods, instructions or products referred to in the content.